Available online at www.sciencedirect.com
ScienceDirect
International Journal of Heat and Fluid Flow 28 (2007) 1092–1097
International Journal of HEAT AND FLUID FLOW
www.elsevier.com/locate/ijhff

A simplified explicit algebraic model for the Reynolds stresses

Marco Antonello [a,*], Massimo Masi [b]

[a] Centre of Studies and Activities for Space, University of Padova, Via Venezia 15, 35131 Padova, Italy
[b] Department of Mechanical Engineering, University of Padova, Via Venezia 1, 35131 Padova, Italy

Received 13 March 2006; received in revised form 27 February 2007; accepted 16 March 2007
Available online 21 May 2007

Abstract

A simplified consistency condition for the production-to-dissipation ratio is developed to obtain an explicit algebraic Reynolds stress model. The stress expression is based on the well-known tensor representation derived from quasi-linear pressure–strain correlation models for two-dimensional mean flows in the weak-equilibrium limit. Results obtained for homogeneous turbulent flows, a backward-facing step flow, and a channel bend flow indicate that the model combines improved accuracy with computational efficiency.

Keywords: Explicit algebraic Reynolds stress models; Weak-equilibrium condition; Consistency condition

1. Introduction

The algebraic Reynolds stress models (ARSMs) were first described by Rodi (1972, 1976). In this formulation an implicit algebraic relation for the Reynolds stress-anisotropy tensor $\mathbf{b}$ is obtained by assuming the weak-equilibrium hypothesis, $D\mathbf{b}/Dt = 0$, by neglecting the diffusion of $\mathbf{b}$, and by including the dissipation rate anisotropy effects in the model of the pressure–strain correlation tensor. Most of the ARSMs use models for the pressure–strain correlation that can be deduced from the quasi-linear relation

$$\begin{aligned}\Pi^* = &-\left(\overline{C}_1 + C_1^*\frac{\mathsf{P}}{\varepsilon}\right)\mathbf{b} + (\overline{C}_2 - C_2^*\mathrm{II}_b^{1/2})\mathbf{s}^* \\ &+ C_3\left(\mathbf{b}\mathbf{s}^* + \mathbf{s}^*\mathbf{b} - \frac{2}{3}tr(\mathbf{b}\mathbf{s}^*)\mathbf{I}\right) \\ &+ C_4[(\boldsymbol{\omega}^* + \boldsymbol{\Omega}^*)\mathbf{b} - \mathbf{b}(\boldsymbol{\omega}^* + \boldsymbol{\Omega}^*)],\end{aligned} \tag{1}$$

where P/ε is the production-to-dissipation ratio, $\bar{C}_i$, C_i^*, and C_i are numerical constants, and $\mathrm{II}_b = b_{ij}b_{ij}$ is the second invariant of the anisotropy tensor. The pressure–strain correlation tensor $\boldsymbol{\Pi}^*$, the mean strain-rate tensor $\mathbf{s}^*$, the mean vorticity tensor $\boldsymbol{\omega}^*$, and the rotation-rate tensor of the non-inertial frame $\boldsymbol{\Omega}^*$ are normalised by the turbulent time scale k/ε. The above assumptions along with model (1) lead to the implicit algebraic equation for $\mathbf{b}$

$$\begin{aligned}&\left(\overline{B}_1 + B_1^*\frac{\mathsf{P}}{\varepsilon}\right)\mathbf{b} \\ &\quad = -(\overline{B}_2 + B_2^*\mathrm{II}_b^{1/2})\mathbf{s}^* - B_3\left(\mathbf{b}\mathbf{s}^* + \mathbf{s}^*\mathbf{b} - \frac{2}{3}tr(\mathbf{b}\mathbf{s}^*)\mathbf{I}\right) \\ &\qquad - B_4(\mathbf{w}^*\mathbf{b} - \mathbf{b}\mathbf{w}^*),\end{aligned} \tag{2}$$

in which $\overline{B}_1 = \overline{C}_1 - 2$, $B_1^* = C_1^* + 2$, $\overline{B}_2 = 4/3 - \overline{C}_2$, $B_2^* = C_2^*$, $B_3 = 2 - C_3$, $B_4 = 2 - C_4$, and $\mathbf{w}^* = \boldsymbol{\omega}^* + \boldsymbol{\Omega}^*(4 - C_4)/(2 - C_4)$ is the mean total normalised vorticity tensor.

The major inconvenience of all traditional implicit algebraic Reynolds stress models, like those of Pope (1975) and Taulbee (1992), lies in the non-linearity of the equation for the production-to-dissipation ratio or for the Reynolds stresses themselves. When these equations are solved multiple solutions or singularities that can occur may cause numerical instability.

Using representation theory and linearising Eq. (2) with prescribed equilibrium values of P/ε and II_b, Gatski and Speziale (1993) obtained an explicit expression of $\mathbf{b}$, which

* Corresponding author. Tel.: +39 049 8276746; fax: +39 049 8276788.

0142-727X/$ - see front matter © 2007 Elsevier Inc. All rights reserved.
doi:10.1016/j.ijheatfluidflow.2007.03.006

Nomenclature

$\mathbf{b} = (2k)^{-1}\boldsymbol{\tau} - (1/3)\mathbf{I}$	Reynolds stress- anisotropy tensor
c_f	skin-friction coefficient
$C_{\varepsilon 1}$, $C_{\varepsilon 2}$	coefficients of transport equation for ε
C_μ	linear term coefficient of $\mathbf{b}$
H, H_s	u-channel height and step height
II_b	second invariant of $\mathbf{b}$
k	turbulent kinetic energy
P	production rate of k
s/H	normalised curvilinear abscissa on the u-channel centre line
$\mathbf{s}^*$	normalised mean strain-rate tensor
t	time
$\bar{u}$, u'	mean and fluctuating streamwise (or longitudinal) velocities
$\overline{u'v'}$	Reynolds shear stress
v'	fluctuating spanwise (or normal) velocity
$\mathbf{w}^*$	normalised mean total vorticity tensor
x/H_s	normalised distance beyond the step
y/H	normalised distance from the inner wall of the bend
y/H_s	normalised distance from the lower wall of the step
Greek symbols	
ε	dissipation rate of k
ζ	second invariant of $\mathbf{w}^*$
η	second invariant of $\mathbf{s}^*$
θ	bend angle measured from its entrance
$\boldsymbol{\Pi}^*$	normalised pressure–strain correlation tensor
$\boldsymbol{\tau}$	Reynolds stress tensor
$\boldsymbol{\Omega}^*$	normalised reference frame rotation-rate tensor
$\boldsymbol{\omega}^*$	normalised mean vorticity tensor

overcomes the aforementioned numerical problems. This expression, which is valid for three-dimensional flows, turns out to be too difficult to use in practical applications because of the ten independent tensor groups needed. Therefore, it is common practice to apply the simpler two-dimensional representation of Gatski and Speziale (1993)

$$\mathbf{b} = -C_\mu\left[\mathbf{s}^* + \frac{B_4}{\overline{B}_1 + 2B_1^* C_\mu \eta}(\mathbf{s}^*\mathbf{w}^* - \mathbf{w}^*\mathbf{s}^*) - \frac{2B_3}{\overline{B}_1 + 2B_1^* C_\mu \eta}\left(\mathbf{s}^{*2} - \frac{1}{3}tr(\mathbf{s}^{*2})\mathbf{I}\right)\right] \tag{3}$$

to three-dimensional flows. Here $\eta = s_{ij}^* s_{ij}^*$ is the second invariant of the non-dimensional strain-rate tensor.

When the methodology of Gatski and Speziale (1993) is used to simulate a turbulent flow far from equilibrium, the resulting Reynolds stress model can be internally inconsistent. For two-dimensional flows, Girimaji (1996) overcame this problem by solving a cubic equation for P/ε. The proper root of this equation has been extracted by Jongen and Gatski (1999) from an analysis of the equilibrium states. However, in practical applications, where complex turbulent flows arise, this approach yields a set of equations that is rather cumbersome to be solved numerically. Wallin and Johansson (2000) derived a simpler cubic equation for P/ε by using the same special assumptions of Taulbee (1992).

The purpose of this work is the development of a simplified equation for P/ε, in order to obtain an explicit algebraic Reynolds stress model (EARSM) that combines improved accuracy with computational efficiency.

2. Simplified consistency condition

The main problem of the explicit relationship (3) is the determination of an expression for C_μ. For two-dimensional mean flows, this is equivalent to finding an equation of the production-to-dissipation ratio since $\mathrm{P}/\varepsilon = 2C_\mu\eta$. Girimaji (1996) obtained an expression for C_μ by imposing the so-called consistency condition for P/ε and by solving the corresponding cubic equation.

An alternative methodology, developed to simplify the expression of C_μ, is described in the following discussion. The equation for P/ε is derived by taking the trace of the product of Eq. (2) with $\mathbf{s}^*$:

$$\frac{1}{2}\left(\overline{B}_1 + B_1^*\frac{\mathrm{P}}{\varepsilon}\right)\frac{\mathrm{P}}{\varepsilon} = \left(\overline{B}_2 + B_2^* II_b^{1/2}\right)\eta - B_3\eta b_{33} + 2B_4 tr(\mathbf{w}^*\mathbf{b}\mathbf{s}^*). \tag{4}$$

A simplified equation for C_μ can be obtained by approximating the stress-anisotropy model (3) as

$$\mathbf{b} = -C_\mu\left[\mathbf{s}^* + \frac{B_4}{\chi_0}(\mathbf{s}^*\mathbf{w}^* - \mathbf{w}^*\mathbf{s}^*) - \frac{2B_3}{\chi_0}\left(\mathbf{s}^{*2} - \frac{1}{3}tr(\mathbf{s}^{*2})\mathbf{I}\right)\right], \tag{5}$$

in which $\chi_0 = \overline{B}_1 + B_1^*(\mathrm{P}/\varepsilon)_0$ depends on the model of the production-to-dissipation ratio $(\mathrm{P}/\varepsilon)_0$. Thus, inserting the approximate model (5) and $\mathrm{P}/\varepsilon = 2C_\mu\eta$ into expression (4) yields, after same manipulations,

$$2B_1^*\chi_0\eta C_\mu^2 + \left[\overline{B}_1\chi_0 - \frac{2}{3}B_3^2\eta + 2B_4^2\zeta - B_2^*(\eta\xi)^{1/2}\right]C_\mu - \overline{B}_2\chi_0 = 0, \tag{6}$$

where $\xi = \chi_0^2 + 2B_4^2\zeta + 2/3B_3^2\eta$. This is a quadratic equation for C_μ, the coefficients of which are functions of the chosen model for $(\mathrm{P}/\varepsilon)_0$, and of the invariants of the strain-rate η and of the total vorticity tensor $\zeta = w_{ij}^* w_{ij}^*$.

The solution of Eq. (6) requires to specify a model for the production-to-dissipation ratio $(\mathrm{P}/\varepsilon)_0$. A functional form for it can be deduced by substituting the quasi-linear

representation of the anisotropy tensor $\mathbf{b} = -C_\mu \mathbf{s}^*$ into Eq. (4) and by assuming a constant value of II_b. In this way, it is a simple matter to obtain the quadratic equation

$$\left(\frac{\mathsf{P}}{\varepsilon}\right)_0^2 + 2A_1\left(\frac{\mathsf{P}}{\varepsilon}\right)_0 - A_0\eta = 0, \tag{7}$$

in which A_0 and A_1 are positive constants. Since one of the two roots of this equation is always non-positive and the other is always non-negative, only the latter can match the values of P/ε in equilibrium homogeneous shear flow and in the log-layer. Hence, the sought functional form is

$$\left(\frac{\mathsf{P}}{\varepsilon}\right)_0 = (A_1^2 + A_0\eta)^{1/2} - A_1. \tag{8}$$

The determination of the two constants A_0 and A_1 is described at the end of this section.

In order to simplify the expression of the roots of Eq. (6), the following coefficients are defined:

$$\begin{aligned}\beta_2 &= 2B_1^*\chi_0\eta, \quad \beta_1 \\ &= \overline{B}_1\chi_0 - \frac{2}{3}B_3^2\eta + 2B_4^2\zeta - B_2^*(\eta\xi)^{1/2}, \quad \beta_0 = \overline{B}_2\chi_0.\end{aligned} \tag{9}$$

Since the most used pressure–strain correlation models (see e.g. Launder et al., 1975; Gibson and Launder, 1978; Speziale et al., 1991) give positive values for $\overline{B}_1$, B_1^*, and $\overline{B}_2$, it follows that $\beta_0 > 0$ and $\beta_2 \geqslant 0$. Thus, the discriminant $\Delta = \beta_1^2 + 4\beta_2\beta_0$ of Eq. (6) is always positive, and the two real roots are:

$$\begin{aligned}C_{\mu 1} &= \frac{2\beta_0}{\beta_1 + \left(\beta_1^2 + 4\beta_2\beta_0\right)^{1/2}}, \\ C_{\mu 2} &= \frac{2\beta_0}{\beta_1 - \left(\beta_1^2 + 4\beta_2\beta_0\right)^{1/2}}.\end{aligned} \tag{10}$$

As for the choice of which of the two roots is to be taken the requirement is invoked that it must never be negative. Since $\Delta^{1/2} \geqslant |\beta_1|$, it follows that $C_{\mu 1} > 0$ and $C_{\mu 2} < 0$, whatever is the sign of β_1; therefore, the only viable expression of C_μ is $C_{\mu 1}$. This relationship has been obtained by satisfying an approximated consistency condition for the production-to-dissipation ratio based on an initial model $(\mathsf{P}/\varepsilon)_0$. In this sense the methodology can be considered semi-iterative, and the whole procedure could be repeated by substituting $C_{\mu 1}$ into $\mathsf{P}/\varepsilon = 2C_\mu\eta$ to obtain a model for $(\mathsf{P}/\varepsilon)_0$. Calculations of some two-dimensional flows have indicated that this approach provides only a slight improvement of the overall predictions, with an appreciable increase in the computational cost. On the other hand, calculations for homogeneous turbulent flow show that a significant increase in accuracy of the normal stress-anisotropy is obtained by simply inserting the model of $(\mathsf{P}/\varepsilon)_0$, deduced from $C_{\mu 1}$, in the expression of χ_0, without repeating the whole procedure. Thus, the final expression for the explicit algebraic stress-anisotropy tensor is:

$$\begin{aligned}\mathbf{b} = &-\frac{2\beta_0}{\beta_1 + (\beta_1^2 + 4\beta_2\beta_0)^{1/2}}\mathbf{s}^* \\ &- \frac{2B_4\beta_0}{\overline{B}_1[\beta_1 + (\beta_1^2 + 4\beta_2\beta_0)^{1/2}] + 4B_1^*\beta_0\eta}(\mathbf{s}^*\mathbf{w}^* - \mathbf{w}^*\mathbf{s}^*). \\ &+ \frac{4B_3\beta_0}{\overline{B}_1[\beta_1 + (\beta_1^2 + 4\beta_2\beta_0)^{1/2}] + 4B_1^*\beta_0\eta}\left(\mathbf{s}^{*2} - \frac{1}{3}\mathrm{tr}(\mathbf{s}^{*2})\mathbf{I}\right)\end{aligned} \tag{11}$$

The values of the constants A_0 and A_1 appearing in Eq. (8) are determined by setting $(\mathsf{P}/\varepsilon)_0 = (C_{\varepsilon 2} - 1)/(C_{\varepsilon 1} - 1)$ for equilibrium homogeneous shear flow and $(\mathsf{P}/\varepsilon)_0 = 1$ in the log-layer, and by calculating the corresponding values of the velocity gradient given by model (11).

3. Applications of the model

The performance of the model is assessed by solving four test cases: two homogenous flows and two complex wall-bounded flows. The stress model is used in conjunction with the SSG pressure–strain correlation model of Speziale et al. (1991), and with the standard transport equations for k and ε of Launder and Spalding (1974). In EARSM calculations, the value of 1.88 for $C_{\varepsilon 2}$, proposed by Girimaji (2000), is adopted. These assumptions yield the following values of the model constants: $\overline{B}_1 = 1.4$, $B_1^* = 3.8$, $\overline{B}_2 = 0.53$, $B_2^* = 1.3$, $B_3 = 0.75$, $B_4 = 1.6$, $A_0 = 0.22$, $A_1 = 0.092$. In wall-bounded flow simulations, the standard wall-function method of Launder and Spalding (1974) is chosen to bridge the semi-viscous sublayer.

The results of an initially isotropic, rotating, homogeneous shear flow are showed in Fig. 1. The temporal development of the turbulence energy and the stress-anisotropy components b_{11} and b_{12} are presented for two different ratios of the reference frame angular speed Ω and mean velocity gradient S:$\Omega/S = 0.25$ and $\Omega/S = 0.5$. The predictions of the proposed model are compared with those of the standard k–ε model, the GS model of Gatski and Speziale (1993), the G model of Girimaji (1996), the SSG second order closure model, and the LES data of Bardina et al. (1983). The results of the present model are very close to those of the G model. Both models reach almost instantaneously the equilibrium value of the SSG model in all cases; whereas the GS model exhibits this behaviour for b_{11} only when $\Omega/S = 0.25$, and for b_{12} only when $\Omega/S = 0.5$. The standard k–ε model, obviously, is not able to distinguish between the different rotation-rates.

Fig. 2 shows the results of a homogeneous turbulent flow subject to a constant mean strain-rate $\bar{s}_{11} = S$. Model predictions are compared to the DNS data of Lee and Reynolds (1985). The results from the present model are very close to those of the G model in this case as well, and, for b_{11} and b_{12}, they grow more quickly towards the DNS values than those of the GS model and the standard k–ε model.

The predictions of the proposed model, the GS model, and the standard k–ε model are next compared with the

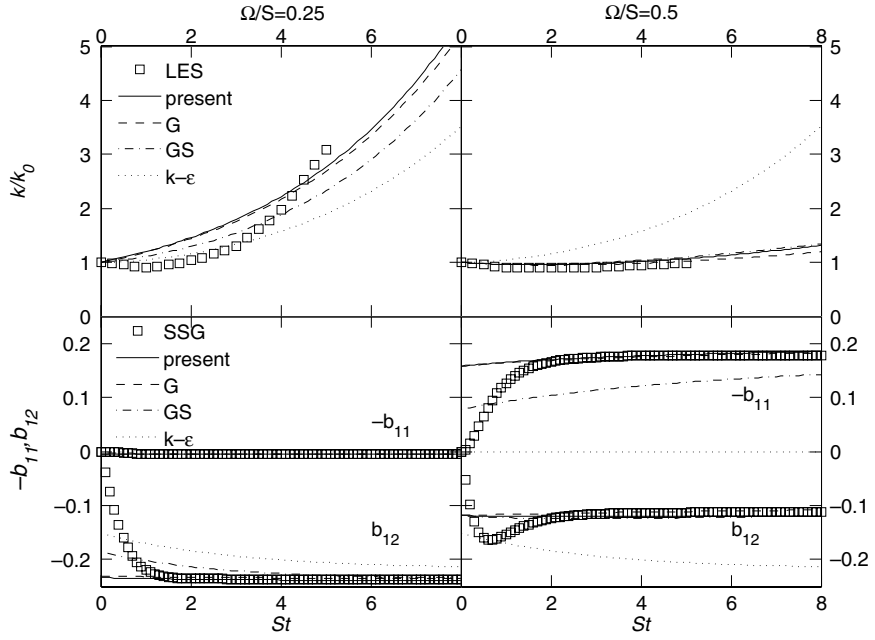

Fig. 1. Time evolution of the turbulent kinetic energy and stress-anisotropies in rotating shear flow for $\varepsilon_0/Sk_0 = 0.296$.

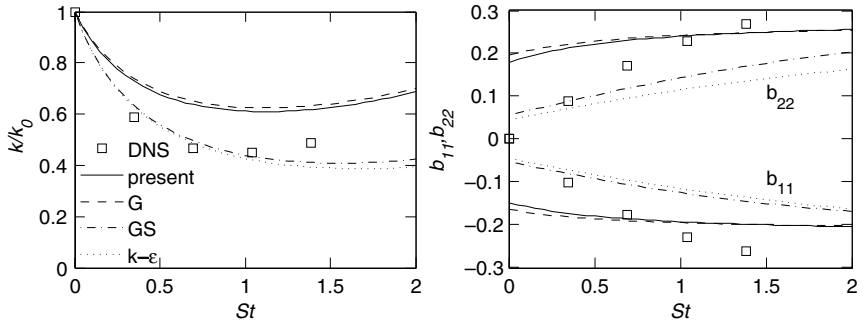

Fig. 2. Time evolution of the turbulent kinetic energy and the stress-anisotropies in plane strain flow for $\varepsilon_0/Sk_0 = 2.0$.

experimental data of the steady, two-dimensional flow over a backward-facing step, in accord with the configuration of Driver and Seegmiller (1985). Fig. 3 shows the distribution of the skin-friction coefficient downstream the step along the lower wall. Both the present model and the GS model underestimate the minimum value of c_f; whereas the standard k–ε model is closer to the measured value. On the other hand, the accuracy of the two EARSMs before the trough is superior. After this peak, the present model gives the better prediction of c_f. The experimental value of the normalised reattachment length is 6.26. The present model, the GS model, and the standard k–ε model predict the following values: 6.24, 6.34 and 5.30, respectively. It is clear that both EARSMs significantly improve the reattachment point results.

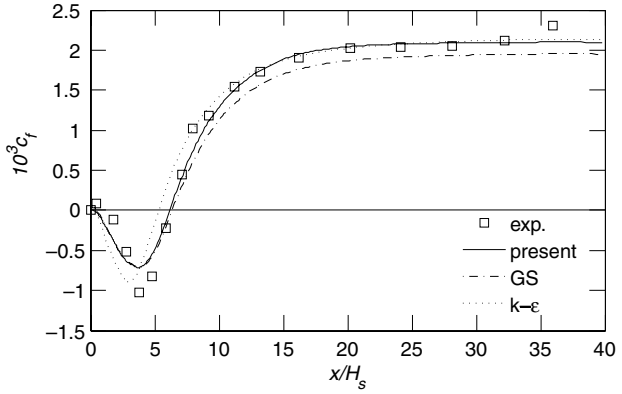

Fig. 3. Skin-friction coefficient distribution along the bottom wall of the backward-facing step.

The profiles of normalised streamwise velocity, turbulence energy, and Reynolds shear stress $\overline{u'v'}$ are shown in Fig. 4. Predictions of the present model and the GS model are very close. Both models predict with more accuracy the reversed flow, but the standard k–ε model performs better in respect of the velocity recovery after the reattachment point. Within the recirculation region, the two explicit algebraic models give distributions of turbulence energy and

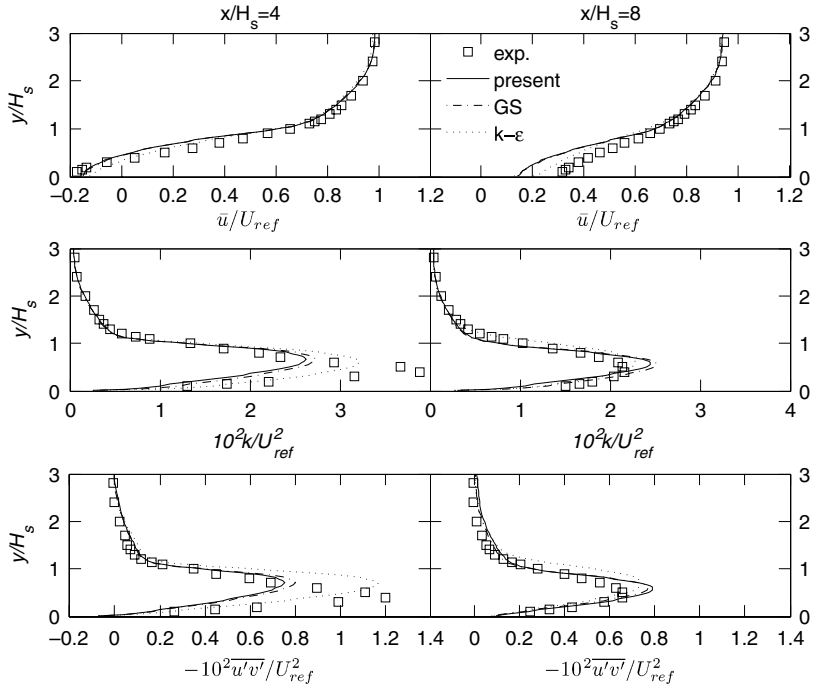

Fig. 4. Streamwise mean velocity and turbulent quantities beyond the step. The turbulence energy is calculated assuming $k = \frac{3}{4}(\overline{u'u'} + \overline{v'v'})$.

Reynolds shear stress that are lower than those of the standard k–ε model. This occurs, because the use of the expression for the variable C_μ decreases the values of the production-to-dissipation ratio and the turbulent viscosity.

The numerical computations with the standard k–ε model, GS model and present model required 1974, 2118 and 2041 iterations, and took 59.1, 63.4 and 59.5 minutes of CPU time on a Intel Xeon 2.2 GHz dual-processor. Despite the more complex formulation, the present model requires a time to convergence 6% lower than the GS model.

The last test case presented is the two-dimensional U-bend in a channel, investigated by Monson and Seegmiller (1992). The distributions of c_f along the inner and the outer walls are compared in Fig. 5. The Results of the present model are almost identical to those of the GS model. Both models predict a late separation near the end of the bend and a reattachment around 1.5 H behind it. After the turn, the two EARSMs provide significant improvement on the standard k–ε model, which predicts a very small separation length and significantly underestimates the maximum c_f value immediately after the concave wall.

Fig. 6 shows the mean longitudinal velocity $\bar{u}$, the turbulence energy k, and the Reynolds shear stress $\overline{u'v'}$, where u' and v' are the longitudinal and the normal instantaneous velocity fluctuations, respectively. At $\theta = 180°$, both EARSMs capture the reversed flow, whereas the standard k–ε model does not. The predictions of k and $\overline{u'v'}$ given by the two algebraic models differ significantly only at $\theta = 90°$. Here, near the convex wall, the k profile given by the present model follows quite well the experimental data; whereas the GS model and the standard k–ε model greatly overestimate the level of k. None of the models is able to capture the measured trend of the turbulent shear stress. Nevertheless, the present model is more sensitive to the curvature effect and predicts a lower level of shear

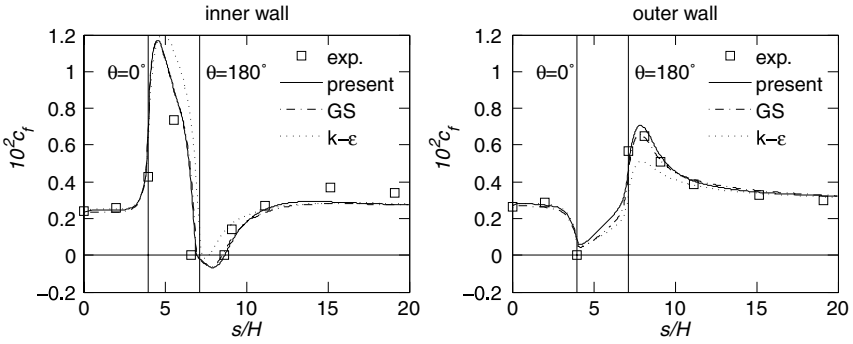

Fig. 5. Skin-friction coefficient distribution along the U-channel walls.

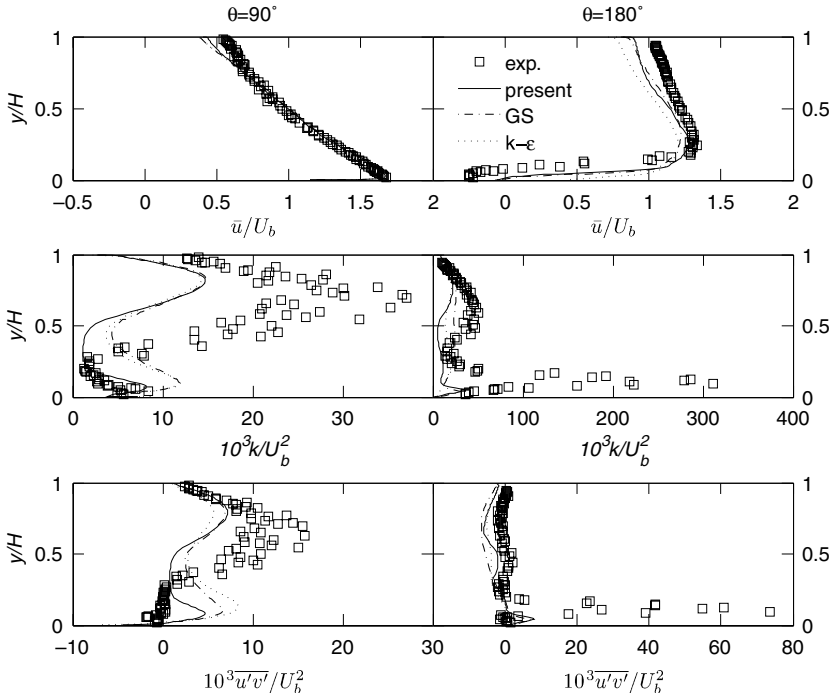

Fig. 6. Longitudinal mean velocity and turbulent quantities in the U-channel. The turbulence energy is calculated assuming $k = \frac{3}{4}(\overline{u'u'} + \overline{v'v'})$.

stress near the inner wall. At $\theta = 180°$ all the models fail to capture the large peaks of the turbulent quantities created by the unsteady separation.

The iterations necessary to reach the convergence with the standard k–ε model, GS model and present model are 1402, 1775 and 1416, and the corresponding time is 42.9, 55.8 and 43.7 min. In this case the present model decreases by 22% the time to convergence of the GS model.

4. Conclusions

An explicit algebraic Reynolds stress model has been developed using an approximate production-to dissipation-ratio consistency condition. Comparison with available data of homogeneous shear flow and plane strain flow shows that the predictions of the present model are very close to those of the Girimaji (1996) model; this means that the physical description has not been affected significantly by the lower order modelling of the equation for production-to-dissipation ratio. Moreover, results for a backward-facing step flow and a channel bend flow show that the model gives some improvements over the model by Gatski and Speziale (1993), with a reduction of the computational cost.

References

Bardina, J., Ferziger, J.H., Reynolds, W.C., 1983. Improved turbulence models based on large-eddy simulation of homogeneous, incompressible turbulent flows. Stanford University Tech. Rep. TF-19.

Driver, D.M., Seegmiller, H.L., 1985. Features of a reattaching turbulent shear layer in divergent channel flow. AIAA J. 23, 163–171.

Gatski, T.B., Speziale, C.G., 1993. On explicit algebraic stress models for complex turbulent flows. J. Fluid Mech. 254, 59–78.

Gibson, M.M., Launder, B.E., 1978. Ground effects on pressure fluctuations in the atmospheric boundary layer. J. Fluid Mech. 86, 491–511.

Girimaji, S.S., 1996. Fully explicit and self-consistent algebraic stress model. Theory Comp. Fluid Dyn. 8, 387–402.

Girimaji, S.S., 2000. Pressure–strain correlation modelling of complex turbulent flows. J. Fluid Mech. 422, 91–123.

Jongen, T., Gatski, T.B., 1999. A unified analysis of planar homogeneous turbulence using single-point closure equations. J. Fluid Mech. 399, 117–150.

Launder, B.E., Spalding, D.B., 1974. The numerical computation of turbulent flows. Comput. Met. Appl. Mech. Eng. 3, 269–289.

Launder, B.E., Reece, G.J., Rodi, W., 1975. Progress in the development of Reynolds stress turbulence closure. J. Fluid Mech. 68, 537–566.

Lee, M.J., Reynolds W.C., 1985. Numerical experiment on the structure of homogeneous turbulence. Stenford University Tech. Rep., TF-24.

Monson, D.J., Seegmiller, H.L., 1992. An experimental investigation of subsonic flow in a two-dimensional u-duct. NASA Technical Memorandum, 103931.

Pope, S.B., 1975. A more general effective-viscosity hypothesis. J. Fluid Mech. 72, 331–340.

Rodi, W., 1972. The prediction of free turbulent boundary layers by use of a two equation model of turbulence. Ph.D. Thesis, University of London, London, England.

Rodi, W., 1976. A new algebraic relation for calculating the Reynolds stresses. Z. Angew. Math., Mech. 56, 219–221.

Speziale, C.G., Sarkar, S., Gatski, T.B., 1991. Modelling the pressure–strain correlation of turbulence: an invariant dynamical systems approach. J. Fluid Mech. 227, 245–272.

Taulbee, D.B., 1992. An improved algebraic Reynolds stress model and corresponding nonlinear stress model. Phys. Fluids A 4, 2555–2561.

Wallin, S., Johansson, A., 2000. An explicit algebraic Reynolds stress model for incompressible and compressible flows. J. Fluid Mech. 403, 89–132.